Rizk et al., http://www.jcb.org/cgi/content/full/jcb.201312039/DC1

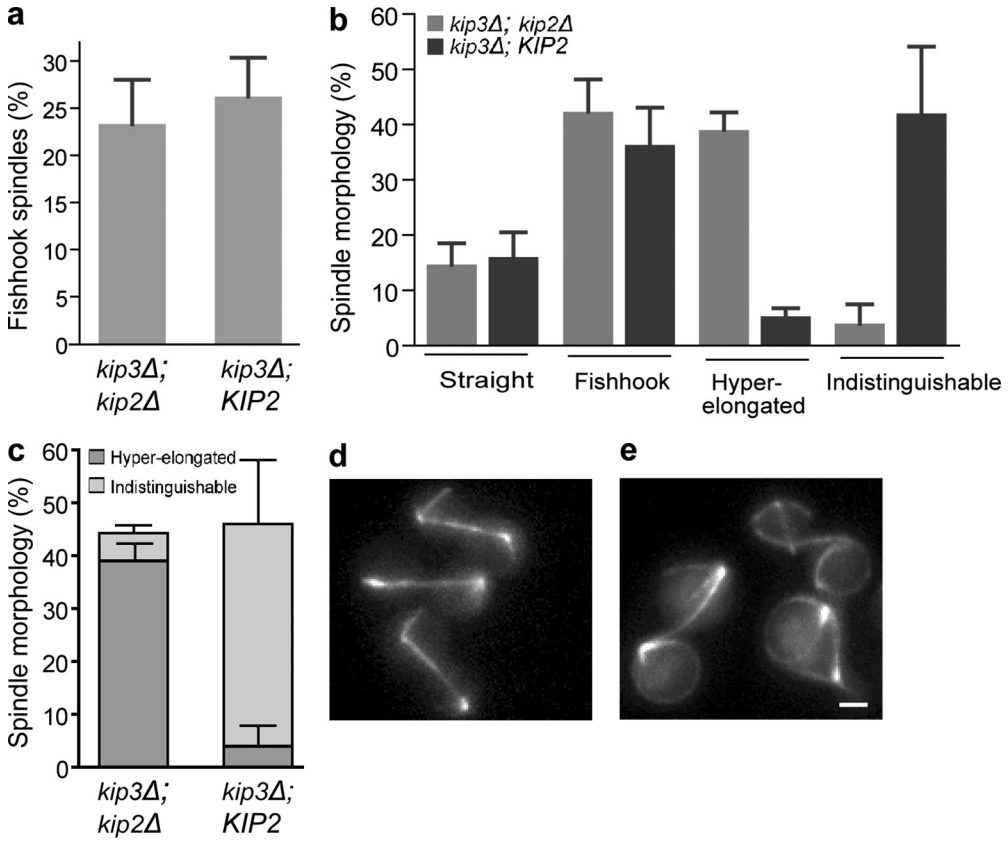

Figure S1. **Kip3 limits anaphase spindle length regardless of genetic background.** (a) The proportion of fishhook spindles in cycling cultures lacking Kip3, either with or without Kip2, was essentially unchanged. The graph shows the average ± SE of three experiments, $n = 69$ for each cell type. (b) Spindle fishhook and hyper-elongation frequencies during anaphase arrest (*cdc15-2*, 2.5 h at 37°C) in *kip3Δ* cells in the presence or absence of Kip2. The frequency of fishhook spindles was similar regardless of whether cells possessed Kip2. The indistinguishable category represents likely hyper-elongated spindles, where spindle length could not be precisely measured due to interference from astral microtubules. The graph shows the average ± SE of three experiments, $n > 300$ for each cell type. (c) Although astral microtubules interfered with accurate length measurements, the total number of hyper-elongated and non-measurable spindles in panel b was also comparable. Thus, removal of Kip2 did not significantly affect spindle length regulation or morphology. (d and e) To ensure that the role of Kip3 in spindle length regulation is not specific to genetic strain or background, we confirmed the result with independently created strains (S288C) as well as a different genetic background (W303). Representative spindle morphology in W303 cells after 2.5 h anaphase arrest with (d) or without (e) Kip3. Bar, 2 µm.

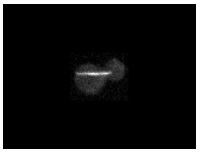

Video 1. **Midzone microtubule dynamics of an elongating anaphase spindle in a control cell.** The video shows fluorescence recovery in a budding yeast spindle midzone after photobleaching GFP-tubulin in a *cdc15-2* cell maintained at 37°C. Pre-bleach and post-bleach frames were extended to allow clear observation. Arrow indicates location of bleached zone. Images were acquired at 5-s intervals using an EM-CCD camera (Cascade 512B; Photometrics) and a spinning-disk confocal attachment (CSU10; Yokogawa Corporation of America) mounted on a microscope (Axiovert 200M; Carl Zeiss). The microscope and photobleaching laser (MicroPoint; Photonics Instruments, Inc.) were controlled by MetaMorph software (Molecular Devices). Playback speed is 15 frames/s.

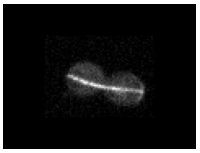

Video 2. **Midzone microtubule dynamics of a full-length anaphase spindle in a control cell.** The video shows fluorescence recovery in a budding yeast spindle midzone after photobleaching GFP-tubulin in a *cdc15-2* cell maintained at 37°C. Pre-bleach and post-bleach frames were extended to allow clear observation. Arrow indicates location of bleached zone. Images were acquired at 5-s intervals using an EM-CCD camera (Cascade 512B; Photometrics) and a spinning-disk confocal attachment (CSU10; Yokogawa Corporation of America) mounted on a microscope (Axiovert 200M; Carl Zeiss). The microscope and photobleaching laser (MicroPoint; Photonics Instruments, Inc.) were controlled by MetaMorph software (Molecular Devices). Playback speed is 15 frames/s.

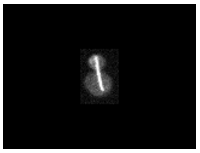

Video 3. **Midzone microtubule dynamics of an elongating anaphase spindle in a *kip3Δ* cell.** The video shows fluorescence recovery in a budding yeast spindle midzone after photobleaching GFP-tubulin in a *kip3Δ cdc15-2* cell maintained at 37°C. Pre-bleach and post-bleach frames were extended to allow clear observation. Arrow indicates location of bleached zone. Images were acquired at 5-s intervals using an EM-CCD camera (Cascade 512B; Photometrics) and a spinning-disk confocal attachment (CSU10; Yokogawa Corporation of America) mounted on a microscope (Axiovert 200M; Carl Zeiss). The microscope and photobleaching laser (MicroPoint; Photonics Instruments, Inc.) were controlled by MetaMorph software (Molecular Devices). Playback speed is 15 frames/s.

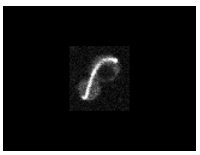

Video 4. **Midzone microtubule dynamics of a full-length anaphase spindle in a *kip3Δ* cell.** The video shows fluorescence recovery in a budding yeast spindle midzone after photobleaching GFP-tubulin in a *kip3Δ cdc15-2* cell maintained at 37°C. Pre-bleach and post-bleach frames were extended to allow clear observation. Arrow indicates location of bleached zone. Images were acquired at 5-s intervals using an EM-CCD camera (Cascade 512B; Photometrics) and a spinning-disk confocal attachment (CSU10; Yokogawa Corporation of America) mounted on a microscope (Axiovert 200M; Carl Zeiss). The microscope and photobleaching laser (MicroPoint; Photonics Instruments, Inc.) were controlled by MetaMorph software (Molecular Devices). Playback speed is 15 frames/s.

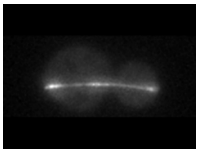

Video 5. **Microtubule plus-end dynamics in a full-length anaphase spindle in a control cell.** The video shows budding yeast spindle microtubules imaged by GFP-tubulin fluorescence in a *cdc15-2* cell maintained at 37°C. Z-plane images spaced 0.4 μm apart, and encompassing the cell, were acquired at 10-s intervals using a CoolSNAP HQ^2 CCD camera (Photometrics) mounted on a microscope (AxioImager M2; Carl Zeiss) driven by SlideBook software (Intelligent Imaging Innovations, Inc.). Maximum intensity Z-projections of each time point are played at 10 frames/s.

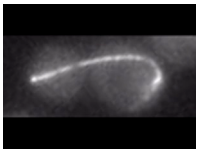

Video 6. **Microtubule plus-end dynamics in a full-length anaphase spindle in a *kip3Δ* cell.** The video shows budding yeast spindle microtubules imaged by GFP-tubulin fluorescence in a *kip3Δ cdc15-2* cell maintained at 37°C. Z-plane images spaced 0.4 μm apart, and encompassing the cell, were acquired at 10-s intervals using a CoolSNAP HQ^2 CCD camera (Photometrics) mounted on a microscope (AxioImager M2; Carl Zeiss) driven by SlideBook software (Intelligent Imaging Innovations, Inc.). Maximum intensity Z-projections of each time point are played at 10 frames/s.

Table S1. **Yeast strains and plasmids used in this study**

Strain name	Mating type	Relevant genotype	Genetic background	Source
MGY960	*MAT*a	*ura3-52::GFP-TUB1-URA3 cdc15-2 his3Δ200 leu2Δ1 trp1Δ63*	S288C	This study
MGY962	*MAT*a	*ura3-52::GFP-TUB1-URA3 cdc15-2 kip3Δ::KanR his3Δ200 leu2Δ1 trp1Δ63*	S288C	This study
MGY963	*MAT*α	*ura3-52::GFP-TUB1-URA3 cdc15-2 kip2Δ::NAT his3Δ200 leu2Δ1 trp1Δ63*	S288C	This study
MGY965	*MAT*α	*ura3-52::GFP-TUB1-URA3 cdc15-2 kip2Δ::NAT kip3Δ::KanR his3Δ200 leu2Δ1 trp1Δ63*	S288C	This study
MGY964	*MAT*a	*ura3-52::GFP-TUB1-URA3 cdc15-2 kip2Δ::NAT his3Δ200 leu2Δ1 trp1Δ63*	S288C	This study
MGY966	*MAT*a	*ura3-52::GFP-TUB1-URA3 cdc15-2 kip2Δ::NAT kip3Δ::KanR his3Δ200 leu2Δ1 trp1Δ63*	S288C	This study
MGY959	*MAT*α	*ura3-52::GFP-TUB1-URA3 cdc15-2 his3Δ200 leu2Δ1 trp1Δ63*	S288C	This study
MGY961	*MAT*α	*ura3-52::GFP-TUB1-URA3 cdc15-2 kip3Δ::KanR his3Δ200 leu2Δ1 trp1Δ63*	S288C	This study
MGY974	*MAT*a	*ura3-52::GFP-TUB1-URA3 cdc15-2 ipl1-321-NAT leu2Δ0 lys2Δ0*	S288C	This study
MGY515	*MAT*α	*ura3::GFP-TUB1-URA3 cdc15-2 his3 leu2 trp1*	W303	This study
MGY679	*MAT*α	*ura3::GFP-TUB1-URA3 cdc15-2 kip3Δ::KanR his3 leu2 trp1*	W303	This study
MGY1282	*MAT*a	*ura3-52::GFP-TUB1-URA3 cdc15-2 stu2-13-URA3 kip2Δ::NAT kip3Δ::KanR leu2Δ1 his3-200 lys2-801*	S288C	This study
MGY361	*MAT*α	pHIS-ceCFP-Tub1-URA3 *cdc15-2 his3Δ200 leu2Δ1 trp1Δ63*	S288C	This study
MGY1528	*MAT*α	*ura3-52::GFP-TUB1-URA3 Ctf3Δ::KanR cdc15-2-NATmx his3Δ1 leu2Δ0 met15Δ0*	S288C	This study
MGY1529	*MAT*α	*ura3-52::GFP-TUB1-URA3 mcm21Δ::KanR cdc15-2-NATmx his3Δ1 leu2Δ0 met15Δ0*	S288C	This study
MGY1530	*MAT*α	*ura3-52::GFP-TUB1-URA3 eaf3Δ::KanR cdc15-2-NATmx his3Δ1 leu2Δ0 met15Δ0*	S288C	This study
MGY1531	*MAT*α	*ura3-52::GFP-TUB1-URA3 mcm16Δ::KanR cdc15-2-NATmx his3Δ1 leu2Δ0 met15Δ0*	S288C	This study
MGY1532	*MAT*α	*ura3-52::GFP-TUB1-URA3 dip5Δ::KanR cdc15-2-NATmx his3Δ1 leu2Δ0 met15Δ0*	S288C	This study
MGY1533	*MAT*α	*ura3-52::GFP-TUB1-URA3 dbf2Δ::KanR cdc15-2-NATmx his3Δ1 leu2Δ0 met15Δ0*	S288C	This study
MGY1534	*MAT*α	*ura3-52::GFP-TUB1-URA3 ylr456wΔ::KanR cdc15-2-NATmx his3Δ1 leu2Δ0 met15Δ0*	S288C	This study
MGY1535	*MAT*a	*ura3-52::GFP-TUB1-URA3 hcm1Δ::KanR cdc15-2 LEU2 trp1Δ63 met15Δ0*	S288C	This study
MGY1536	*MAT*a	*ura3-52::GFP-TUB1-URA3 chl4Δ::KanR cdc15-2 MET15 LEU2 trp1Δ63*	S288C	This study
MGY1537	*MAT*α	*ura3-52::GFP-TUB1-URA3 eaf6Δ cdc15-2 MET15 LEU2 TRP1*	S288C	This study
MGY1538	*MAT*α	*pHIS-ceCFP-Tub1-URA3 cdc15-2 ASE1-3xYFP-LEU2 kip2Δ::NAT his3Δ200 trp1Δ63*	S288C	This study
MGY1539	*MAT*a	*pHIS-ceCFP-Tub1-URA3 cdc15-2 ASE1-3xYFP-LEU2 kip3Δ::KanR kip2Δ::NAT his3Δ200 trp1Δ63*	S288C	This study
MGY1540	*MAT*a	*pHIS-ceCFP-Tub1-URA3 cdc15-2 KIP3-EYFP::HIS kip2Δ::NAT his3Δ200 trp1Δ63*	S288C	This study
MGY1464	*MAT*α	*pHIS-ceCFP-Tub1-URA3 cdc15-2 KIP3-CC-EYFP::LEU2 kip2Δ::NAT his3Δ200 trp1Δ63*	S288C	This study

Plasmid name	Description and markers	Source
pAFS125	GFP-TUB1-URA3, *ampR*	(Straight et al., 1997)
pMG3	GFP-TUB1-LEU2, *ampR*	(Gupta et al., 2002)
pAG25	natMX4, *ampR*	(Goldstein and McCusker, 1999)

References

Goldstein, A.L., and J.H. McCusker. 1999. Three new dominant drug resistance cassettes for gene disruption in *Saccharomyces cerevisiae*. *Yeast*. 15:1541–1553. http://dx.doi.org/10.1002/(SICI)1097-0061(199910)15:14<1541::AID-YEA476>3.0.CO;2-K

Gupta, M.L. Jr., C.J. Bode, D.A. Thrower, C.G. Pearson, K.A. Suprenant, K.S. Bloom, and R.H. Himes. 2002. beta-Tubulin C354 mutations that severely decrease microtubule dynamics do not prevent nuclear migration in yeast. *Mol. Biol. Cell*. 13:2919–2932. http://dx.doi.org/10.1091/mbc.E02-01-0003

Straight, A.F., W.F. Marshall, J.W. Sedat, and A.W. Murray. 1997. Mitosis in living budding yeast: anaphase A but no metaphase plate. *Science*. 277:574–578. http://dx.doi.org/10.1126/science.277.5325.574